In Vitro Identification and Electrophysiological Characterization of Dopamine Neurons in the Ventral Tegmental Area

Tao A. Zhang, **Andon N. Placzek**, and **John A. Dani**
Department of Neurscience Menninger Dept. of Psychiatry & Behavioral Sciences Baylor College of Medicine Houston, Texas, USA

Abstract

Dopamine (DA) neurons in the ventral tegmental area (VTA) have been implicated in brain mechanisms related to motivation, reward, and drug addiction. Successful identification of these neurons *in vitro* has historically depended upon the expression of a hyperpolarization activated current (I_h) and immunohistochemical demonstration of the presence of tyrosine hydroxylase (TH), the rate-limiting enzyme for DA synthesis. Recent findings suggest that electrophysiological criteria may be insufficient for distinguishing DA neurons from non-DA neurons in the VTA. In this study, we sought to determine factors that could potentially account for the apparent discrepancies in the literature regarding DA neuron identification in the rodent brain slice preparation. We found that confirmed DA neurons from the lateral VTA generally displayed a larger amplitude I_h relative to DA neurons located in the medial VTA. Measurement of a large amplitude I_h (> 100 pA) consistently indicated a dopaminergic phenotype, but nondopamine neurons also can have Ih current. The data also showed that immunohistochemical TH labeling of DA neurons can render false negative results after relatively long duration (> 15 min) whole-cell patch clamp recordings. We conclude that whole-cell patch clamp recording in combination with immunohistochemical detection of TH expression can guarantee positive but not negative DA identification in the VTA.

Keywords

Dopaminergic; midbrain; tyrosine hydroxylase; immunohistochemistry; patch clamp recording

1. Introduction

Dopaminergic neurons of the VTA are known to have important roles in motivation and reward. The prevailing view is that activity of these neurons encodes incentive salience and/or perceived environmental deviation from expected reward (Robinson and Berridge, 2000, 2008;Schultz, 2006;Schultz et al., 1997). A change from tonic to phasic firing patterns in these neurons has been suggested to be a crucial signal underlying reward learning (Schultz, 2006). This shift from tonic to phasic firing has been demonstrated to be sufficient for place preference conditioning *in vivo* (Tsai et al., 2009). In addition to their normal physiological roles, these same DA neurons are directly or indirectly targeted by addictive drugs (Dani and Harris,

Address all correspondences to John A. Dani, Department of Neuroscience, Baylor College of Medicine, Houston, TX 77030-3498, Tel (713)798-3710, jdani@bcm.tmc.edu .

2005;Hyman et al., 2006;Kauer and Malenka, 2007;Koob and Nestler, 1997;Volkow et al., 2007). By a variety of differing mechanisms, addictive drugs increase the release of DA from these neurons, particularly in the nucleus accumbens (NAc) (Koob and Nestler, 1997). It has been proposed that when addictive drugs increase DA release in this circuit, they are effectively hijacking a system that normally serves to increase the likelihood of survival (Kauer and Malenka, 2007).

Molecular and immunohistochemical evidence has indicated multiple subpopulations of neurons within the VTA, including DAergic, GABAergic, and more recently glutamatergic (Van Bockstaele and Pickel, 1995; Steffensen et al., 1998; Klink et al., 2001; Chuhma et al., 2004; Korotkova et al., 2004; Margolis et al., 2006; Yamaguchi et al., 2007; Nair-Roberts et al., 2008; Hnasko et al., 2010). In addition to these discrete neuronal subgroups, there is also evidence for co-release of both DA and glutamate primarily from the medial VTA neurons (Chuhma et al., 2004; Hnasko et al., 2010).

Early *in vitro* studies that focused on histochemically identified neurons indicated that DA neurons in the lateral VTA region were more likely to demonstrate a hyperpolarization activated current (I_h) under voltage clamp (Grace and Onn, 1989; Johnson and North, 1992). Later studies confirmed this basic relationship between the DAergic phenotype and I_h (Ford et al., 2006; Klink et al., 2001; Korotkova et al., 2004; Labouebe et al., 2007; Lammel et al., 2008), but another study was unable to find a consistent electrophysiological correlate of DAergic phenotype using immunohistochemistry (Margolis et al., 2006). An important finding was that the magnitude of I_h expression varied according to both the projection target and anatomical subregion within the VTA (Ford et al., 2006; Lammel et al., 2008). These studies suggested that I_h was better suited as an electrophysiological marker of DAergic phenotype when neurons were selected from the lateral portion of the VTA.

Because of the controversy in the literature, we sought to address two specific questions. First, does the expression of I_h vary within confirmed VTA DA neurons as a function of their location on the mediolateral axis? Second, what factors can account for apparent discrepancies in the literature regarding *in vitro* electrophysiological markers of the DA neuron subpopulations within the VTA? Using a combination of immunohistochemistry, transgenic expression of reporter genes, single cell RT-PCR, and electrophysiological recordings, we found a strong relationship between the presence of large amplitude I_h and molecular indicators of the DA phenotype. Our data also showed that under our whole-cell patch clamp conditions, TH immunohistochemical labeling of confirmed DA neurons can render false negative results. As the length of recording in whole-cell increased, false negative TH results increased in likelihood.

2. Methods

2.1 Midbrain slice electrophysiology

All experiments were carried out in accordance with the National Institutes of Health guidelines for the care and use of Laboratory animals (NIH Publications No. 8023, revised 1978) and were approved by the Baylor College of Medicine Institutional Animal Care and Use Committee. Horizontal slices (220 μm thick) containing VTA, hippocampus and substantia nigra pars compacta (SNc) were cut from 17-25 day old C57BL mice, or transgenic mice in which DA neurons were labeled with enhanced green fluorescent protein (EGFP; mouse strain name, STOCK Tg(Th-EGFP)1Gsat/Mmnc) using previously described patch clamp methods (Wooltorton et al., 2003). Briefly, the mice were anesthetized before decapitation, and slices were cut in ice-cold, oxygenated cutting solution containing (in mM) NaCl, 120; NaHCO$_3$, 25; KCl, 3.3; NaH$_2$PO$_4$, 1.23; MgSO$_4$, 2.4; CaCl$_2$, 1.2; dextrose, 10. The slices were incubated at 32 °C for 20mins and then were kept at room temperature (24 °C) for use during a period of

less than 5 hours. Slices were transferred to a recording chamber and continuously perfused with artificial cerebral spinal fluid (ACSF) at 32 °C and a flow rate of 1.5~2 ml/min. The recording ACSF buffer is different from cutting solution in the concentration of Mg^{2+} (0.9 mM) and Ca^{2+} (2 mM). All efforts were made to reduce the number of animals used and to minimize animal suffering in this study.

Recording pipettes were made from thin-walled borosilicate glass (TW150F-4, WPI, Sarasota, FL, 1.5-2.2 MΩ) and filled with 7 μl intracellular solution: (in mM): KCl, 120; EGTA, 0.2; HEPES, 10; $MgCl_2$, 2; 280-290 mOsm, pH 7.2 with KOH in RNase-free water. Cells were voltage clamped at −60 mV after break-in, then switched to current clamp to record neuron firing with a current step protocol (−300pA to 500 pA in 50 pA steps, 2 s duration). Recordings were then switched back to voltage clamp mode and the cell was again held at −60 mV. I_h was recorded with a voltage step protocol (−40 mV to −120 mV in 10 mV steps, 1.5 s duration). All calculations of the peak I_h amplitude were taken from a −60 mV to −120 mV hyperpolarizing step. For current clamp mode, recordings were digitized at 20 kHz and filtered at 10 kHz; for voltage clamp mode, recordings were digitized at 10 kHz, and filtered at 1 kHz.

Midbrain neurons were visualized under infrared light with Nomarski optics (Zeiss, Thornwood, NY). For EGFP-labeled neurons, cells were also visualized by switching light (480nm/520nm: EX/EM), and recordings were made from both EGFP-labeled and non-labeled neurons within the VTA. The lateral VTA was identified as medial to the medial terminal nucleus of the accessory optic tract (MT) and lateral and rostral to the crest of the medial lemniscus (see Fig. 1A). Previous work by Ford, et al. (2006) found that DA neurons that were medial to the crest of the medial lemniscus had a smaller I_h than those that were lateral and rostral to the ML. In horizontal brain sections, the crest of the medial lemniscus (ML) provides a convenient anatomical landmark to separate the lateral from the medial VTA. While this is a somewhat conservative anatomical selection criterion, this method provides a good electrophysiological separation between the two subregions of the VTA.

2.2 Single cell multiplex RT-PCR

Cell cytoplasm was harvested into the recording pipette by applying negative pressure at the end of whole-cell recordings under visual control, and the input resistance was monitored during the aspiration procedure. Only cells without a large change in input resistance (< 20%) were accepted. An outside-out patch was formed by slowly withdrawing the pipette. Then the patch was broken by gently tapping the pipette holder, and the pipette was immediately removed from the recording chamber and inserted into a PCR tube containing 2 μl RNase inhibitor (Ambion). The tip of the electrode was broken at the tip by hitting the bottom of the collection tube, and positive pressure was applied to the back of the pipette to expel the contents of the pipette into the RNase inhibitor solution. Reverse transcription was carried out by using oligo-dT primer (1μl), random hexamer primer (1μl), and M-MLV reverse transcriptase (1μl, 200U) at 42 °C for 50 min. The cDNA was stored at −20 °C before amplification.

A multiplex PCR with "nested" primer design was used to amplify the target sequences, which included two markers for DA neurons (tyrosine hydroxylase, TH, and the dopamine transport protein, DAT), two markers for GABAergic cells (GAD65 and GAD67) and the house keeping gene GAPDH. All targeted genes were then simultaneously amplified by adding "outer" primer pairs of all target genes into individual PCR tubes containing the cDNAs from a single cell (final volume 76 μl per tube). The first amplification round was performed with PTC-100 (MJ Research, Waltham, MA) and consisted of 2 min at 95 °C followed by 20 cycles (95 °C for 15 sec, 54 °C for 30 sec, 72 °C for 30 sec) and a final 10 min elongation at 72 °C. Then, 1 μl of the product of the first PCR was used in the second amplification round to amplify individual genes by adding only the specific "inner" primer pairs into each tube (final volume 25 μl). The second amplification round consisted of 95 °C for 2 min followed by 30 cycles (95 °C for 15

sec, 59 °C for 30 sec, 72 °C for 30 sec) and 7 min elongation at 72 °C. The products of the second PCR were analyzed in 2.5% agarose gels and stained with ethidium bromide.

The "outer" primers were the following:

Gene Primers (from 5′ to 3′) Sense Antisense Fragment size (bp)

DAT	TGCTGGTCATTGTTCTGCTC	AAGACAACGAAGCCAGAGGA	(361)
TH	GTACATCCGTCATGCCTCCT	TACACAGCCCAAACTCCACA	(203)
GAD65	GGGGCTTTTGATCCTCTCTT	CCACATGGCGTCCACACT	(328)
GAD67	GTGCAGGCTACCTCTTCCAG	CACCATCGAAAACCATCTCA	(228)
GAPDH	AACTTTGGCATTGTGGAAGG	CCCTGTTGCTGTAGCCGTAT	(472)

The "inner" primers were the following:

Gene Primers (from 5′ to 3′) Sense Antisense Fragment size (bp)

DAT	TGTGAGGCATCTGTGTGGAT	GCTCGTCAGGGAGTTAATGG	(156)
TH	CTGGGACACGTACCCATGTT	GAACCAGTACACCGTGGAGA	(120)
GAD65	GATGTCCCGGAAACACAAGT	CTGCATCAGTCCCTCCTCTC	(133)
GAD67	ACAAGGCGATTCAGTGTGG	AGCTCCAGGCATTTGTTGAT	(109)
GAPDH	GTGTTCCTACCCCCAATGTG	GGTCCTCAGTGTAGCCCAAG	(138)

2.3 Immunohistochemistry

TH-EGFP mice were intracardically perfused with ice-cold phosphate buffer for 3 to 5 min before switching to 4% paraformaldehyde PBS buffer for 5-10 min circulation. The brain was removed and fixed in 4% paraformaldehyde solution in a glass bottle overnight at 4 °C. Brain tissue was cut horizontally in 50μm sections on a vibratome and rinsed in phosphate buffer. Slices were then preincubated in a blocking solution containing 3% normal donkey solution and 0.3% triton X-100 for 2 h before slices were incubated with polyclonal antibody against TH (1:1000, AB1542, Chemicon) overnight at 4 °C. After washing with PBS, slices were treated with a secondary Cy3-conjugated donkey antisheep IgG (1:1000, Jackson ImmunoResearch). No TH immunoreactivity was found when only the secondary antibody was applied. Native EGFP expressed in transgenic mouse neurons were directly excited without the use of antibodies.

For TH and neurobiotin double labeling, the recording pipette contained 0.3% neurobiotin and was gently withdrawn from the cell at the end of recording. Slices were immediately transferred to 4% paraformaldehyde and processed using the same procedures described above except for the addition of AMCA-conjugated streptavidin (1:1000, Jackson ImmunoResearch) during the secondary antibody treatment step.

2.4 Statistical analysis

Values are presented as mean ± SEM. Statistical significance was assessed by using Student's unpaired t-test or one-way ANOVA, and $p < 0.05$ was accepted as statistical significance.

3. Results

3.1 Confirmation of dopaminergic phenotype by single cell RT-PCR and immunohistochemistry in TH-EGFP mice

We used the crest of the medial lemniscus to divide the VTA into lateral and medial regions, and DA neurons were selected from both the lateral and medial VTA (Fig. 1A). Using immunohistochemical methods we labeled TH in transgenic mice designed to express enhanced green fluorescent protein (EGFP) coupled to the TH promoter (Fig. 1B). In slices containing the VTA from transgenic mice, all EGFP positive cells were also labeled by the TH antibody (592 cells, 5 mice). Of the cells positively labeled with the TH antibody, 65 ± 3 % were also EGFP positive. This result is consistent with reports using similar transgenic mouse models showing that not all TH-positive neurons are labeled by EGFP (Matsushita et al., 2002). Therefore, all EGFP-positive neurons were found to be TH-positive, indicating that both EGFP and TH could be used to identify DA neurons.

Using single-cell RT-PCR, we found that all EGFP expressing cells tested were also positive for TH mRNA (Fig. 1B&C; 21/21 of cells, 100% success rate for mRNA harvest). Unlike TH mRNAs, the DAT RT-PCR signal was a less consistent indicator of DA phenotype than TH. Several cells were TH positive and DAT negative, but the results suggest that the DAT signal was below our level of detection in those cases. During each recording day, RT-PCR positive and negative controls were performed. Positive controls included recording and harvesting mRNAs from known cell types. For example, after recordings from cells in the VTA, we also recorded from interneurons at the border of the hilus and granule cell layer in the hippocampal dentate gyrus where the cells are primarily GABAergic, and from cells in the substantia nigra pars compacta (SNc) where the vast majority of the cells are putative DA neurons. These types of positive controls gave positive bands on markers of either GABA for dentate interneurons (n = 11) or DA for SNc putative DA neurons (n = 6) but not both. Negative controls included samples of RNase-free water and intracellular recording solution instead of cytoplasm contents. This type of negative control was never positive on any target genes throughout the experiment. Additional negative controls were also performed randomly by using ACSF from the recording chamber in the presence of slices and by non-specifically harvesting slice tissue when a recording electrode was inserted into the tissue and retrieved without forming a seal or suction. These types of random controls occasionally gave positive bands for the housing keeping gene GAPDH only, but always gave negative readings for GABA or DA. Taken together, these data indicate that the single cell RT-PCR method did not yield false positive signals in detecting the DA phenotype in the midbrain.

3.2 Electrophysiological properties of confirmed DA neurons from the lateral VTA

Having established both the reliability and accuracy of the single-cell RT-PCR method for determining the neuronal DA phenotype in TH-EGFP mice, we then used single-cell RT-PCR in C57BL/6 mice to identify a population of neurons that contained TH mRNAs, but were negative for the GABAergic cell markers GAD65 and GAD67 mRNAs (Fig. 2A&B). Whole-cell voltage clamp recordings from these neurons display a characteristically large hyperpolarization activated current (I_h) (Fig. 2C). We harvested cytoplasm from 92 cells, and 34 cells (37%) displayed no positive bands for either GABA markers or DA markers, but were positive for GAPDH. This result suggests that the content of the mRNA harvested from these cells might be below the detection threshold of our single-cell RT-PCR method, or that these unidentified cells could be another cell phenotype in the VTA other than GABA or DA. Because we could not be certain of the neurotransmitter type for these unidentified neurons, we expected them to be a mixed collection of cell types and did not use this group in comparisons.

We also found that 4 cells (4.3%) displayed a dual DA/GABA identity, an observation that was previously reported by groups using similar techniques in rats (Guyon et al., 1999; Klink et al., 2001). Surprisingly, although our technique for identifying the GABA phenotype has been confirmed in hippocampal GABA interneurons, only 2 of the 92 cells we harvested from the VTA showed positive markers for GABA. Although there may have been a small number of GABA neurons in the VTA of C57 mice, it seems more likely that the low success rate of identifying GABA cells by single cell RT-PCR arose because an insufficient amount of GAD mRNA was harvested by the recording pipette. To increase our chance of recording from GABA neurons in the VTA, we harvested cytoplasm from non-fluorescent neurons in TH-EGFP mice, but this did not increase the number of cells expressing GABAergic markers. This result might be explained by the fact that the EGFP positive cells account for approximately 65% of the total number of DA neurons in the VTA (Fig. 1), and this may not sufficiently increase the probability of avoiding DA neurons in the effort to select GABA neurons preferentially.

The rest of the 52 cells (57%) were TH mRNA-positive but GAD mRNA-negative. Among the confirmed DA neurons, 16 were located in the lateral VTA and 19 were located in the medial VTA (for the remaining 17 confirmed DA neurons, no effort was made to record their relative position within the VTA). All cells in the lateral VTA displayed an I_h, and most cells (14/16) showed a large I_h that was > 100 pA (Fig. 2C&G). By contrast, while all confirmed DA neurons (19/19) of the medial VTA displayed I_h, relatively few showed an I_h greater than 100 pA (6/19) (Fig. 2E&G). These data show that DA neurons in the lateral VTA display a substantially larger amplitude of I_h than those in the medial VTA (lateral, 313 ± 41 pA vs. medial, 88 ± 19 pA, $p < 0.001$, Fig. 2C&E), consistent with the findings from other researchers (Ford et al., 2006; Lammel et al., 2008). Previous reports have used an I_h "negative" or "positive" classification scheme, which can result in ambiguity. In this manuscript we have quantified all hyperpolarization-activated currents, no matter how small. While the I_h shown in Fig. 2E is very small, it is not zero. These results are a reason why we have suggested the use of a I_h amplitude threshold (100 pA). Corresponding to the expression of I_h, under current clamp, lateral VTA DA neurons also show a larger voltage "sag" than those in the medial VTA (Fig. 2D&F, bottom traces) (sag ratio: 0.51 vs. 0.34, $p < 0.001$).

Another characteristic feature of DA neurons in the lateral VTA is the spike frequency adaptation that occurs when depolarized (lateral, Fig. 2D and medial, Fig. 2F, top traces). In addition to the difference in I_h and sag ratio, the DA neurons in the lateral VTA display larger membrane capacitance (lateral, 76.9 ± 3.5 vs. medial, 54.3 ± 4.5, $p < 0.001$) and a smaller input resistance (lateral, 224.8 ± 15.3 vs. medial, 397.1 ± 67.6, $p < 0.05$), suggesting that the DA cells in the lateral VTA have a larger surface area.

3.3 Immunohistochemical labeling of DA neurons shows variable TH signals

In DA neurons from TH-EGFP transgenic mice (Fig. 3), we saw that the probability of observing a positive immunohistochemical TH signal varied with the length of whole-cell patch clamp recordings. In whole-cell recordings that were less that 3 minutes in length (Fig. 3 upper) from confirmed DA neurons (EGFP, green) that also were back-filled with neurobiotin (NB, blue), 87.5 % (14/16 cells) were also TH immunoreactive (TH, red). By contrast, if the recording duration was greater than 15 minutes, only 20% (2/10 cells) showed a positive TH signal by immunohistochemistry. The missing TH label is indicated by a white arrow in Figure 3. This false negative for TH suggests that under the whole-cell recording conditions we used, particularly in the case of relatively long whole-cell recordings, TH immunohistochemistry can commonly yield false negatives and be insufficient as a sole standard for identification of the DA phenotype.

4. Discussion

The DA neurons of the ventral midbrain have projections that are organized in a topographical hierarchy (Conrad et al., 2008; Ikemoto, 2007). For example, neurons in the medial region project to the medial portion of the NAc, while those of the more lateral areas tend to project to the lateral NAc and the basolateral amygdala (Ford et al., 2006; Ikemoto, 2007; Lammel et al., 2008). Moving even further laterally and dorsally into the substantia nigra pars compacta (SNc), the DA projections extend largely to the dorsal striatum (Ikemoto, 2007). The DA target regions of the ventral and dorsal striatum have recurrent inhibitory projections to the midbrain DA neurons, and based on in vitro and in vivo evidence, this hierarchical anatomical organization underlies a behavioral progression from the signaling of incentive salience to habit learning (Conrad et al., 2008; Luscher and Bellone, 2008). While there is a growing body of literature describing the basic function of these DA neurons under both normal and abnormal conditions, there is still much that remains unknown about their functional properties and their roles in reward learning. Furthermore, because of their importance in behavior, disease, and addiction, DA neurons remain prime targets for therapeutic intervention.

Since DA neurons were discovered as a distinct subset of neurons in the ventral midbrain, there have been multiple reports attempting to classify and identify them based on a variety of physiological, pharmacological, and anatomical parameters (Bjorklund and Dunnett, 2007; Grace and Bunney, 1995). Much of the early characterization work focused on the DA neurons of the SNc, and subsequent studies suggested a less homogenous population of DA neurons in the VTA (Ford et al., 2006; Lammel et al., 2008). As more studies of DA neurons of the VTA emerged, our understanding of the characteristic features of this subset of cells was expanded and refined. It is becoming increasingly clear that certain DA neurons in the medial VTA region nearer to the midline have distinct properties from those that lie more laterally or in the SNc. Subgroups of DA neurons within the medial VTA are not always sensitive to D2 receptor agonists (Chiodo et al., 1984; Lammel et al., 2008), which have been used widely as pharmacological indicators of DA neurons (Grace and Bunney, 1985; White and Wang, 1984). Furthermore, recent work has demonstrated that many medial VTA DA neurons may also release glutamate as a co-transmitter (Chuhma et al., 2009; Chuhma et al., 2004; Descarries et al., 2008; Hnasko et al., 2010; Kawano et al., 2006).

Although similar in many ways, each of these various DA neuron subgroups has somewhat different electrophysiological and pharmacological properties. For example, our results showed that the DA neurons of the medial VTA tend to have smaller amplitude I_h, whereas those of the lateral VTA near the medial border of the SNc tend to display a large I_h, supporting earlier findings (Ford et al., 2006; Lammel et al., 2008; Sarti et al., 2007). The difference in the amplitude of I_h expression may complicate the use of what has historically been used as an electrophysiological marker of the DA phenotype. This raises the issue of potential problems associated with the use of an I_h "positive" or "negative" DA neuron classification scheme. Thus, even though confirmed VTA DA neurons can have relatively low I_h amplitudes, our data indicate that it much better to adopt selection criteria that favor large I_h (> 100 pA). Our data also support the use of I_h mainly in the lateral region of the VTA where I_h amplitudes tend to be higher. Additional use of molecular markers is recommended when using I_h for DA identification in the medial VTA.

Immunohistochemistry is commonly used to identify cells with various neurotransmitter phenotypes. Here we showed that under our recording conditions it is possible to observe no immunohistochemical labeling of neurons that were identifiable as dopaminergic by unambiguous alternative methods. Obtaining false negatives is particularly true for whole-cell patch clamp recordings that lasted for longer than 15 minutes under our experimental conditions. It is possible that TH may decline owing to the whole-cell patch configuration as

internal solution exchanges with the cytoplasm. In addition, there may be leakage after the patch pipette is withdrawn. Antibodies raised against different epitopes or other species might provide better labeling for a longer time course and decrease false negative results. Our data suggest, however, that for experiments involving relatively long-duration whole-cell recordings, immunohistochemical methods should be corroborated by additional methods to identify DA neurons. Since prolonged recordings may result in false negative identification, a positive identification with immunohistochemical methods was found to be reliable.

Although VTA DA neurons have been extensively studied, there is comparatively less information about the other types of midbrain neurons such as the GABA and glutamate subpopulations. The quantity of GABA neurons in the VTA is estimated to be around 30-35%, and the glutamate neurons account for about 2% (Kalivas, 1993; Nair-Roberts et al., 2008). Consequently, there is also relatively little information about how to distinguish these types of neurons in an in vitro brain slice experiment. Although not thoroughly studied, it has been reported that immunohistochemistry using various commercially available GAD antibodies for midbrain slices is not effective (Nair-Roberts et al., 2008; Olson and Nestler, 2007). We also did not obtain good labeling using GAD immunohistochemistry in midbrain slices, but we did using cortical or hippocampal slices. We attempted single-cell RT-PCR as an alternative to confirm GABAergic phenotype in the VTA in C57 wild type mice, but our results showed that the probability of successfully identifying GABA neurons in the VTA is very low. Single-cell RT-PCR was successfully used to identify GABAergic interneurons in the hilar region in the hippocampal dentate gyrus, where these cells have a large soma and have been well characterized. The two GAD positive neurons we collected from the VTA had smaller somata than the DA neurons, consistent with studies using in situ hybridization and immunohistochemistry (Ford et al., 1995; Nair-Roberts et al., 2008). The small soma of VTA GABA neurons could potentially contribute to the difficulty in RT-PCR identification by failing to provide sufficient amounts of cytoplasm containing GAD65/67 mRNAs compared to cells with larger somata.

Even though we report a 100% correlation between the expression of TH mRNA and the EGFP positive neurons in the transgenic mice, without direct evidence of other neurotransmitters in the TH mRNA-negative neurons, we cannot reasonably conclude that all TH-negative cells from C57 mice are non-DA neurons. The TH immunohistochemistry data (Fig. 1) indicate a population of EGFP-negative DA neurons. There is a possibility that the EGFP-positive cells in the transgenic mice have higher levels of TH-mRNA than a putative population of EFGP-negative DA neurons.

These data support previous studies examining electrophysiological and molecular identification of VTA DA neurons (Ford et al., 2006; Klink et al., 2001; Korotkova et al., 2004; Labouebe et al., 2007; Lammel et al., 2008). Taken together the results suggest that I_h is a useful electrophysiological marker of VTA DA neurons, but I_h is rendered much less reliable in the medial VTA owing to its smaller and more variability amplitude. Additional measures should be taken for identification of DA neurons in the more medial regions of the VTA. Furthermore, TH immunohistochemistry is a useful tool for the identification of DA neurons when a strong positive label is obtained. However, the absence of TH label can be a false negative result, especially when long lasting whole-cell patch clamp experiments are conducted.

Acknowledgments

References

1. Bjorklund A, Dunnett SB. Dopamine neuron systems in the brain: an update. Trends Neurosci 2007;30:194–202. [PubMed: 17408759]

2. Chiodo LA, Bannon MJ, Grace AA, Roth RH, Bunney BS. Evidence for the absence of impulse-regulating somatodendritic and synthesis-modulating nerve terminal autoreceptors on subpopulations of mesocortical dopamine neurons. Neuroscience 1984;12:1–16. [PubMed: 6462443]

3. Chuhma N, Choi WY, Mingote S, Rayport S. Dopamine neuron glutamate cotransmission: frequency-dependent modulation in the mesoventromedial projection. Neuroscience 2009;164:1068–1083. [PubMed: 19729052]

4. Chuhma N, Zhang H, Masson J, Zhuang X, Sulzer D, Hen R, Rayport S. Dopamine neurons mediate a fast excitatory signal via their glutamatergic synapses. J Neurosci 2004;24:972–981. [PubMed: 14749442]

5. Conrad KL, Tseng KY, Uejima JL, Reimers JM, Heng LJ, Shaham Y, Marinelli M, Wolf ME. Formation of accumbens GluR2-lacking AMPA receptors mediates incubation of cocaine craving. Nature 2008;454:118–121. [PubMed: 18500330]

6. Dani JA, Harris RA. Nicotine addiction and comorbidity with alcohol abuse and mental illness. Nat Neurosci 2005;8:1465–1470. [PubMed: 16251989]

7. Descarries L, Berube-Carriere N, Riad M, Bo GD, Mendez JA, Trudeau LE. Glutamate in dopamine neurons: synaptic versus diffuse transmission. Brain Res Rev 2008;58:290–302. [PubMed: 18042492]

8. Ford B, Holmes CJ, Mainville L, Jones BE. GABAergic neurons in the rat pontomesencephalic tegmentum: codistribution with cholinergic and other tegmental neurons projecting to the posterior lateral hypothalamus. J Comp Neurol 1995;363:177–196. [PubMed: 8642069]

9. Ford CP, Mark GP, Williams JT. Properties and opioid inhibition of mesolimbic dopamine neurons vary according to target location. J Neurosci 2006;26:2788–2797. [PubMed: 16525058]

10. Grace AA, Bunney BS. Low doses of apomorphine elicit two opposing influences on dopamine cell electrophysiology. Brain Res 1985;333:285–298. [PubMed: 3995296]

11. Grace, AA.; Bunney, BS. Electrophysiological Properties of Midbrain Dopamine Neurons. In: Bloom, FE.; Kupfer, DJ., editors. Psychopharmacology: The fourth generation of progress. Raven Press; New York: 1995. p. 163-177.

12. Grace AA, Onn SP. Morphology and electrophysiological properties of immunocytochemically identified rat dopamine neurons recorded in vitro. J Neurosci 1989;9:3463–3481. [PubMed: 2795134]

13. Guyon A, Laurent S, Paupardin-Tritsch D, Rossier J, Eugene D. Incremental conductance levels of GABAA receptors in dopaminergic neurones of the rat substantia nigra pars compacta. J Physiol 1999;516(Pt 3):719–737. [PubMed: 10200421]

14. Hnasko TS, Chuhma N, Zhang H, Goh GY, Sulzer D, Palmiter RD, Rayport S, Edwards RH. Vesicular glutamate transport promotes dopamine storage and glutamate corelease in vivo. Neuron 2010;65:643–656. [PubMed: 20223200]

15. Hyman SE, Malenka RC, Nestler EJ. Neural mechanisms of addiction: the role of reward-related learning and memory. Annu Rev Neurosci 2006;29:565–598. [PubMed: 16776597]

16. Ikemoto S. Dopamine reward circuitry: two projection systems from the ventral midbrain to the nucleus accumbens-olfactory tubercle complex. Brain Res Rev 2007;56:27–78. [PubMed: 17574681]

17. Johnson SW, North RA. Two types of neurone in the rat ventral tegmental area and their synaptic inputs. J Physiol 1992;450:455–468. [PubMed: 1331427]

18. Kalivas PW. Neurotransmitter regulation of dopamine neurons in the ventral tegmental area. Brain Res Brain Res Rev 1993;18:75–113. [PubMed: 8096779]

19. Kauer JA, Malenka RC. Synaptic plasticity and addiction. Nat Rev Neurosci 2007;8:844–858. [PubMed: 17948030]

20. Kawano M, Kawasaki A, Sakata-Haga H, Fukui Y, Kawano H, Nogami H, Hisano S. Particular subpopulations of midbrain and hypothalamic dopamine neurons express vesicular glutamate transporter 2 in the rat brain. J Comp Neurol 2006;498:581–592. [PubMed: 16917821]

21. Klink R, de Kerchove d'Exaerde A, Zoli M, Changeux JP. Molecular and physiological diversity of nicotinic acetylcholine receptors in the midbrain dopaminergic nuclei. J Neurosci 2001;21:1452–1463. [PubMed: 11222635]

22. Koob GF, Nestler EJ. The neurobiology of drug addiction. J Neuropsychiatry Clin Neurosci 1997;9:482–497. [PubMed: 9276849]

23. Korotkova TM, Ponomarenko AA, Brown RE, Haas HL. Functional diversity of ventral midbrain dopamine and GABAergic neurons. Mol Neurobiol 2004;29:243–259. [PubMed: 15181237]

24. Labouebe G, Lomazzi M, Cruz HG, Creton C, Lujan R, Li M, Yanagawa Y, Obata K, Watanabe M, Wickman K, Boyer SB, Slesinger PA, Luscher C. RGS2 modulates coupling between GABAB receptors and GIRK channels in dopamine neurons of the ventral tegmental area. Nat Neurosci 2007;10:1559–1568. [PubMed: 17965710]

25. Lammel S, Hetzel A, Hackel O, Jones I, Liss B, Roeper J. Unique properties of mesoprefrontal neurons within a dual mesocorticolimbic dopamine system. Neuron 2008;57:760–773. [PubMed: 18341995]

26. Luscher C, Bellone C. Cocaine-evoked synaptic plasticity: a key to addiction? Nat Neurosci 2008;11:737–738. [PubMed: 18575469]

27. Margolis EB, Lock H, Hjelmstad GO, Fields HL. The ventral tegmental area revisited: is there an electrophysiological marker for dopaminergic neurons? J Physiol 2006;577:907–924. [PubMed: 16959856]

28. Matsushita N, Okada H, Yasoshima Y, Takahashi K, Kiuchi K, Kobayashi K. Dynamics of tyrosine hydroxylase promoter activity during midbrain dopaminergic neuron development. J Neurochem 2002;82:295–304. [PubMed: 12124430]

29. Nair-Roberts RG, Chatelain-Badie SD, Benson E, White-Cooper H, Bolam JP, Ungless MA. Stereological estimates of dopaminergic, GABAergic and glutamatergic neurons in the ventral tegmental area, substantia nigra and retrorubral field in the rat. Neuroscience 2008;152:1024–1031. [PubMed: 18355970]

30. Olson VG, Nestler EJ. Topographical organization of GABAergic neurons within the ventral tegmental area of the rat. Synapse 2007;61:87–95. [PubMed: 17117419]

31. Robinson TE, Berridge KC. The psychology and neurobiology of addiction: an incentive-sensitization view. Addiction 2000;95(Suppl 2):S91–117. [PubMed: 11002906]

32. Robinson TE, Berridge KC. Review. The incentive sensitization theory of addiction: some current issues. Philos Trans R Soc Lond B Biol Sci 2008;363:3137–3146. [PubMed: 18640920]

33. Sarti F, Borgland SL, Kharazia VN, Bonci A. Acute cocaine exposure alters spine density and long-term potentiation in the ventral tegmental area. Eur J Neurosci 2007;26:749–756. [PubMed: 17686047]

34. Schultz W. Behavioral theories and the neurophysiology of reward. Annu Rev Psychol 2006;57:87–115. [PubMed: 16318590]

35. Schultz W, Dayan P, Montague PR. A neural substrate of prediction and reward. Science 1997;275:1593–1599. [PubMed: 9054347]

36. Tsai HC, Zhang F, Adamantidis A, Stuber GD, Bonci A, de Lecea L, Deisseroth K. Phasic firing in dopaminergic neurons is sufficient for behavioral conditioning. Science 2009;324:1080–1084. [PubMed: 19389999]

37. Volkow ND, Fowler JS, Wang GJ, Swanson JM, Telang F. Dopamine in drug abuse and addiction: results of imaging studies and treatment implications. Arch Neurol 2007;64:1575–1579. [PubMed: 17998440]

38. White FJ, Wang RY. Pharmacological characterization of dopamine autoreceptors in the rat ventral tegmental area: microiontophoretic studies. J Pharmacol Exp Ther 1984;231:275–280. [PubMed: 6491980]

39. Wooltorton JR, Pidoplichko VI, Broide RS, Dani JA. Differential desensitization and distribution of nicotinic acetylcholine receptor subtypes in midbrain dopamine areas. J Neurosci 2003;23:3176–3185. [PubMed: 12716925]
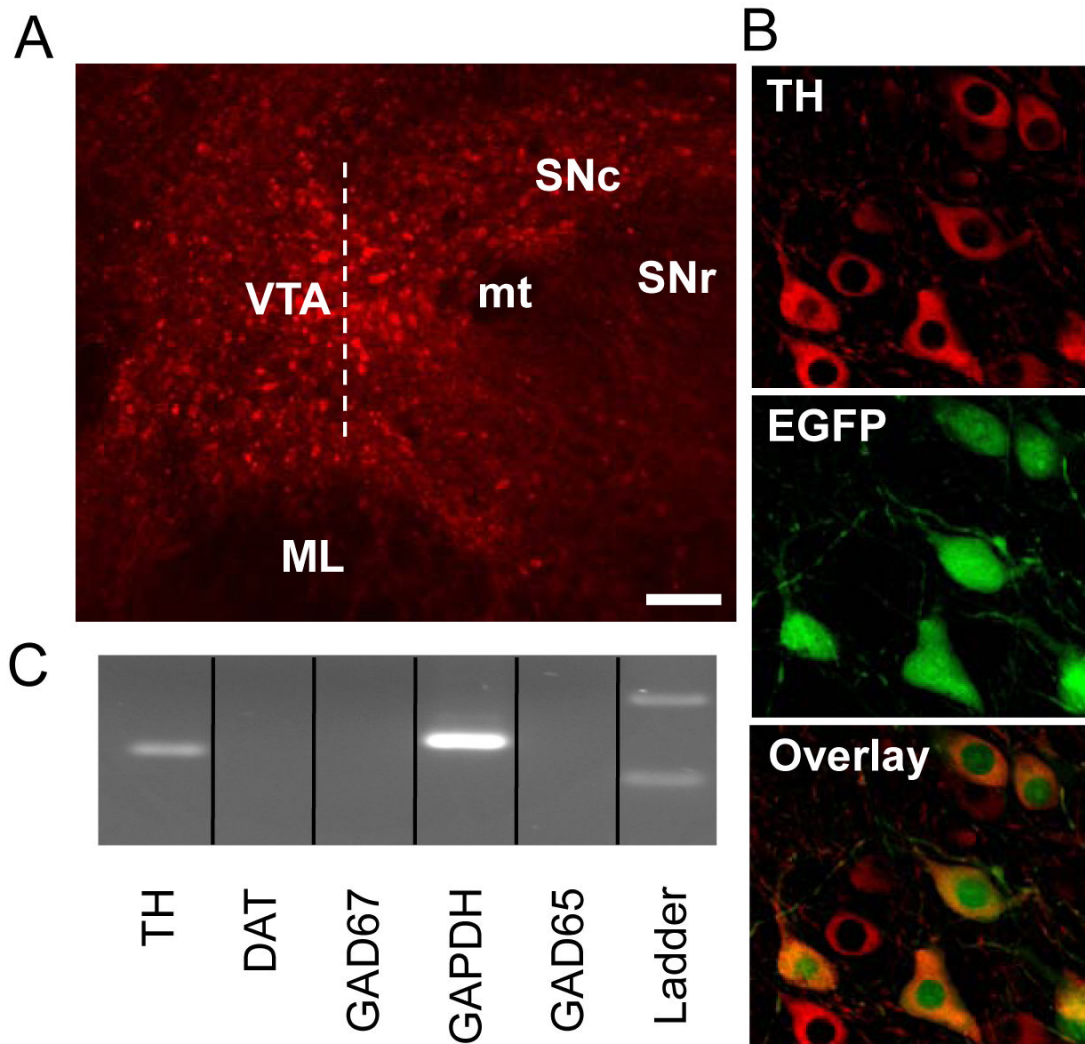
Fig. 1.
Determination of the DA phenotype using single cell RT-PCR and immunohistochemistry. A) Representative mouse horizontal brain slice showing the VTA and surrounding anatomical features. The dashed line extending along the rostrocaudal axis from the crest of the medial lemniscus (ML) indicates the boundary between "lateral" and "medial" VTA regions used in this study. The scale bar represents 70 μm. Abbreviations: VTA = ventral tegmental area, SNc = substantia nigra pars compacta, SNr = substantia nigra pars reticulate, ML = medial lemniscus, mt = medial terminal nucleus of the accessory optic tract. B) The DA phenotype in TH-EGFP mice was confirmed by TH immunohistochemistry. All EGFP expressing cells were also co-labeled with the TH antibody, but not TH-positive neurons contain EGFP. C) The single-cell RT-PCR method confirmed that all EGFP positive cells tested were also positive for TH mRNA, but negative for GAD65 or GAD67 mRNAs.
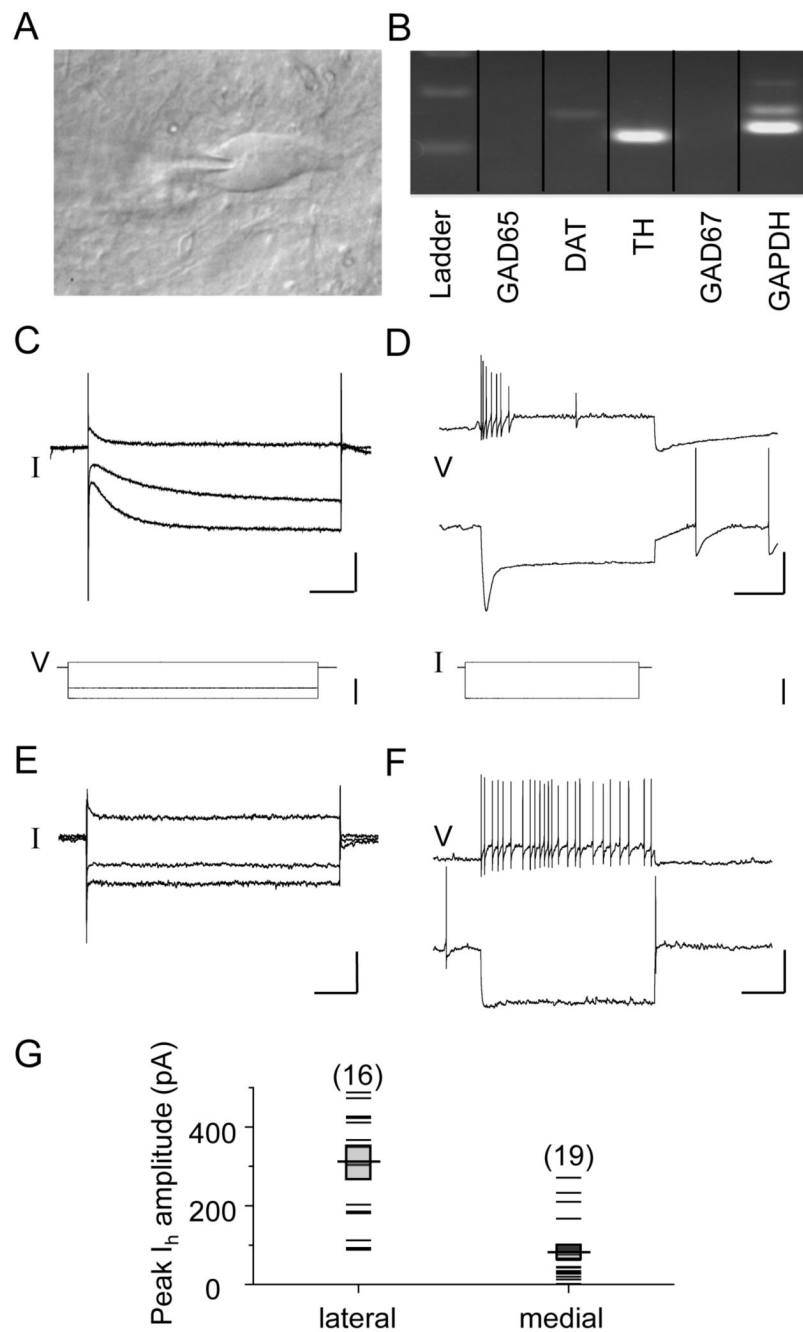
Fig. 2.
Electrophysiological properties of confirmed DA neurons from the lateral and medial VTA.
A) An infrared differential interference contrast image showing the bipolar morphology of a representative DA neuron in the lateral VTA. At the end of each electrophysiological recording, cytosol was harvested by gentle aspiration for single-cell RT-PCR characterization. B) Representative results from a single-cell RT-PCR reaction confirming the DA phenotype of the cell shown in panel A. C) Raw data traces under voltage clamp mode depicting a large hyperpolarization activated current (I_h) during whole-cell voltage clamp recording from a neuron in the lateral VTA. Scale bars = 250 pA/0.25 ms. Lower traces represent the voltage steps applied to activate I_h. Scale bar = 50 mV. D) Raw data traces generated under current

clamp mode from the same cell as in panel C showing spike frequency adaptation when the cell membrane was depolarized, and a large voltage "sag" when hyperpolarized. Scale bars = 40 mV/0.5 ms. Lower traces represent the current steps applied to activate the voltage "sag". Scale bar = 0.5 nA. E) Raw data traces depicting a very small hyperpolarization activated current (I_h) during whole-cell voltage clamp recording from a confirmed DA neuron in the medial VTA. Scale bars = 250 pA/0.25 ms. F) Raw data traces generated under current clamp mode from the same cell as in panel E showing little or no spike frequency adaptation when the cell membrane was depolarized, and a very small voltage "sag" when hyperpolarized. Scale bars = 40 mV/0.5 ms. G) Scatter plots showing the I_h peak amplitude for confirmed DA neurons recorded from lateral and medial VTA. Mean peak I_h (horizontal line) and s.e.m. (shaded transparent box) are superimposed.
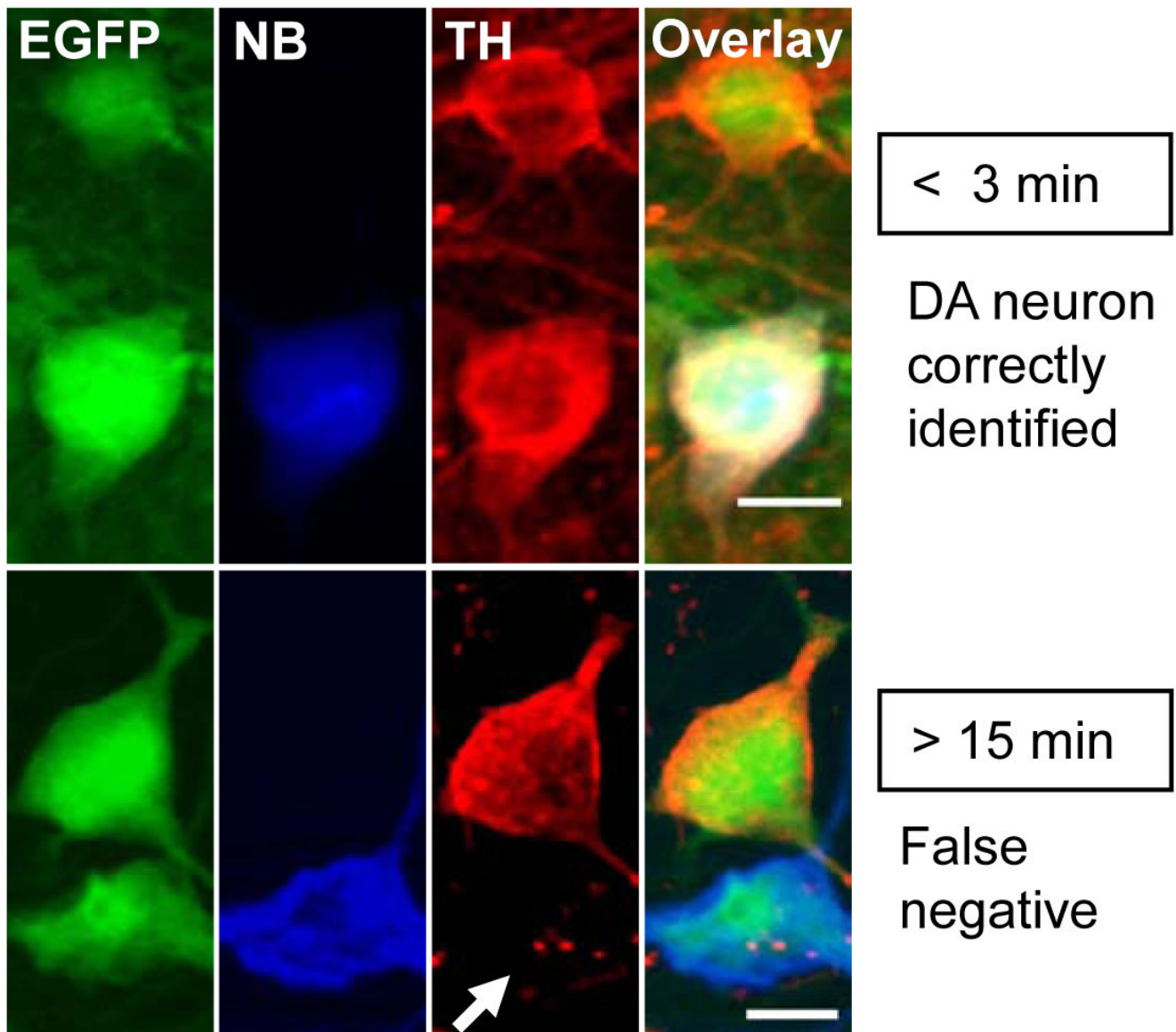
Fig. 3.
Immunohistochemical labeling of identified DA neurons showing TH signals are affected by the length of whole-cell patch clamp recordings. EGFP labeling (green) in transgenic mice identifies neurons as dopaminergic. Neurons that were whole-cell patch clamped were backfilled by including neurobiotin (NB) in the recording pipette and were NB-positive (blue). TH immunohistochemistry routinely labeled the EGFP positive neurons when the whole-cell recordings were < 3 min (TH, red, upper panel). But, after > 15 min of whole-cell recording, EGFP neurons were frequently not labeled (8 out of 10) by TH immunohistochemistry (white arrow indicating false negative, lower panel).